

## Supplementary information

for

### **Design and simulation of biomimetic microfluidic designs to achieve uniform flow and DNA capture for high-throughput multiplexing**

Enas Osman<sup>1</sup>, Jonathan L'Heureux-Hache<sup>2</sup>, Phoebe Li<sup>2</sup>, Leyla Soleymani<sup>1,2,3,4\*</sup>

<sup>1</sup> School of Biomedical Engineering, McMaster University, Hamilton L8S 4L8, Ontario, Canada.

<sup>2</sup> Department of Engineering Physics, McMaster University, Hamilton L8S 4L8, Ontario, Canada

<sup>3</sup> Michael G. DeGroot Institute for Infectious Disease Research, McMaster University, Hamilton L8S 4L8, Ontario, Canada

<sup>4</sup> Department of Biochemistry and Biomedical Sciences, McMaster University, Hamilton L8S 4L8, Ontario, Canada.

\* Corresponding author

Email: [soleyml@mcmaster.ca](mailto:soleyml@mcmaster.ca)

## Supplementary methods

**Peclet number (Pe)<sup>1</sup>:** Pe is a dimensionless parameter that quantifies the balance between convective and diffusive transport. It is defined in terms of the velocity of the fluid in the reaction sites from simulation ( $u$ ), hydraulic diameter ( $D_h$ ), and diffusivity ( $D$ ), as represented by (1).

$$Pe = \frac{u \times D_h}{D} \quad (1)$$

**Diffusion coefficient (D)<sup>2</sup>:** D is calculated using Stokes-Einstein equation, where  $D$  is the diffusion coefficient in m<sup>2</sup>/s,  $k_B$  is the Boltzmann constant ( $1.38 \times 10^{-23}$  J/K) relating to the average kinetic energy of DNA to the temperature of the system  $T$  (310.15° K),  $\eta$  is the dynamic viscosity in Pa.s, and  $r$  is the radius of the diffusing target (short ssDNA = 2.2 nm)<sup>3</sup>.

$$D = \frac{k_B \times T}{6\pi\eta r} \quad (2)$$

## Supplementary tables

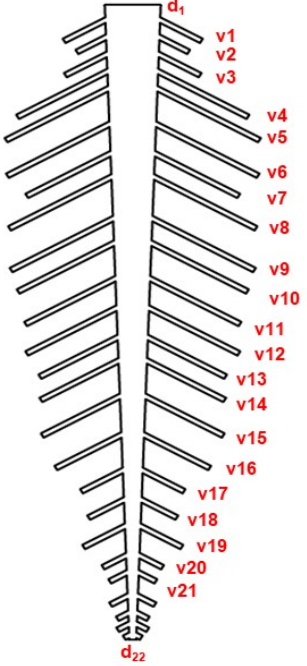
Table S1: Simulation parameters used in COMSOL Multiphysics models (laminar flow, transport of diluted species, and surface reactions).

Simulation parameters	Values	[Ref]
Flow rates	10, 50, 100 $\mu\text{L}/\text{min}$	4, 5
Target concentrations	1, 10, 50, 100 nM	6
$k_{\text{off}}$	$0.09 \text{ min}^{-1}$	6
$k_{\text{on}}$	$0.96 \times 10^6 \text{ M}^{-1} \text{ min}^{-1}$	6
Probe density	$4.55 \times 10^{12} \text{ molecules}/\text{cm}^2$	6
Dynamic viscosity ( $\mu$ ) – water	0.001 Pa.s	1
Density $\rho$ – water	1000 $\text{kg}/\text{m}^3$	1
Diffusion coefficient – water	$1 \times 10^{-9} \text{ m}^2/\text{s}$	1
Dynamic viscosity ( $\mu$ ) – plasma	0.0012 Pa.s	7
Density $\rho$ – plasma	1030 $\text{kg}/\text{m}^3$	7
Diffusion coefficient – plasma	$5.29 \times 10^{-11} \text{ m}^2/\text{s}$	Equation (4)
Dynamic viscosity ( $\mu$ ) – blood	0.006 Pa.s	7
Density $\rho$ – blood	1080 $\text{kg}/\text{m}^3$	7
Diffusion coefficient – blood	$1.72 \times 10^{-11} \text{ m}^2/\text{s}$	Equation (4)
Dynamic viscosity ( $\mu$ ) – Saliva	0.008 Pa.s	8
Density $\rho$ – Saliva	1012 $\text{kg}/\text{m}^3$	9
Diffusion coefficient – Saliva	$1.49 \times 10^{-11} \text{ m}^2/\text{s}$	Equation (4)

Table S2: Estimated transverse diameter and length of vertebral bony segments of the healthy human spine, along with the scaled and optimized dimensions of the spine-inspired design.

Vertebrae	Transverse diameter (mm)	Length (mm)	Scaled diameter ( $\mu\text{m}$ )	Scaled length ( $\mu\text{m}$ )	Width ( $\mu\text{m}$ )	Optimized width ( $\mu\text{m}$ )	
	C1	115	32	115	32	-	-
	C2	123	32	123	32	100	98.5
	C3	131	28	131	28	100	100
	C4	133	27	133	27	100	100
	C5	131	27	131	270	100	100
	C6	121	26	121	26	100	100
	T1	11	31	110	31	100	101
	T2	108	34	108	34	100	105
	T3	97	37	97	37	100	105
	T4	95	37	95	37	100	110
	T5	92	39	92	39	100	113.5
	T6	88	39	88	39	100	117.5
	T7	84	42	84	42	100	122.3
	T8	83	43	83	43	100	127.5
	T9	86	45	86	45	100	132.7
	T10	86	46	86	46	100	138.6
	T11	82	48	82	48	100	142.5
	T12	86	51	86	51	100	150
	L1	94	54	94	54	100	153.5
	L2	71	57	71	57	100	149.3

Table S3: Measured staghorn sumac veins network, along with scaled and optimized dimensions for the leaf-inspired design.



Vein #	Vein length (mm)	Scaled vein length ( $\mu\text{m}$ )	Optimized vein length ( $\mu\text{m}$ )	Vein separation distance (d) ( $\mu\text{m}$ )	Optimized vein separation distance (d) ( $\mu\text{m}$ )
1	700	700	1700	500	480.3
2	1500	1500	1700	200	189.5
3	1700	1700	1700	200	189.5
4	1700	1700	1690	200	189.5
5	1400	1400	1640	500	489.7
6	1700	1700	1615	400	389.6
7	1700	1700	1600	300	289.6
8	1600	1600	1555	600	589.7
9	1500	1500	1520	400	309.6
10	1500	1500	1470	500	489.7
11	1300	1300	1425	400	389.6
12	1300	1300	1360	400	389.6
13	1300	1300	1310	300	289.6
14	1100	1100	1250	500	489.7
15	700	700	1120	550	539.7
16	600	600	1010	500	489.7
17	700	700	870	400	389.6
18	400	400	750	350	340
19	300	300	590	400	389.6
20	300	300	510	200	189.5
21	200	200	380	300	389.6
22	-	-	-	-	565.8

Table S4: Coefficient of variance percentage of the simple branched design under fully developed laminar flow for various DNA target concentrations (100, 50, 10, 1 nM) under different flow rates (100, 50, 10  $\mu\text{L}/\text{min}$ ).

Simple branched Time (min)	100 $\mu\text{L}/\text{min}$				50 $\mu\text{L}/\text{min}$				10 $\mu\text{L}/\text{min}$			
	100 nM	50 nM	10 nM	1 nM	100 nM	50 nM	10 nM	1 nM	100 nM	50 nM	10 nM	1 nM
0.34	82.93	82.98	83.03	83.77	94.09	94.16	94.29	92.20	124.29	121.81	124.54	118.98
0.66	71.21	71.23	71.26	71.14	81.64	81.68	81.74	79.02	108.81	106.33	108.90	104.15
1.30	60.29	60.03	162.97	162.97	70.23	163.54	163.19	159.98	94.79	160.54	163.58	157.86
2.58	52.49	52.99	175.09	175.56	62.39	171.68	173.87	171.66	85.75	169.74	174.70	169.47
5.14	42.12	43.30	125.95	124.49	52.37	148.97	126.47	122.96	74.88	126.65	127.82	122.40
10.26	27.42	29.30	31.97	32.43	38.62	58.26	42.76	39.98	61.39	60.88	65.28	60.03
20.50	13.39	15.83	22.15	23.02	23.06	34.44	31.83	29.98	46.96	48.32	54.14	49.07
36.50	9.20	11.13	14.19	14.90	11.63	22.92	19.31	18.78	32.62	34.79	41.25	36.74
52.50	7.02	8.45	9.81	10.49	6.36	10.88	9.98	10.47	20.88	22.66	29.23	25.64
68.50	3.73	4.76	6.74	7.25	3.60	6.39	5.66	6.14	12.03	13.72	19.53	16.95
84.50	1.50	1.99	3.32	3.65	2.17	4.07	3.45	3.49	6.73	8.18	12.81	11.10
100.50	0.76	0.81	1.05	1.18	1.16	2.27	1.87	1.76	4.05	5.21	8.68	7.64
116.50	0.51	0.53	0.47	0.43	0.48	1.18	0.87	0.80	2.73	3.64	6.16	5.55
132.50	0.27	0.33	0.37	0.35	0.18	0.52	0.33	0.31	1.98	2.66	4.49	4.14
148.50	0.11	0.15	0.19	0.20	0.12	0.09	0.12	0.13	1.65	1.96	3.32	3.11
164.50	0.05	0.05	0.08	0.09	0.07	0.06	0.09	0.09	1.39	1.55	2.63	2.45

Table S5: Coefficient of variance percentage over time of the original spine-inspired design under fully developed laminar flow for various DNA target concentrations (100, 50, 10, 1 nM) under different flow rates (100, 50, 10  $\mu\text{L}/\text{min}$ ).

Original spine Time (min)	100 $\mu\text{L}/\text{min}$				50 $\mu\text{L}/\text{min}$				10 $\mu\text{L}/\text{min}$			
	100 nM	50 nM	10 nM	1 nM	100 nM	50 nM	10 nM	1 nM	100 nM	50 nM	10 nM	1 nM
0.34	8.10	8.18	8.28	9.21	15.13	15.44	15.29	15.55	45.97	49.12	49.20	48.40
0.66	0.64	0.64	0.63	0.86	1.72	1.72	1.67	1.86	24.71	27.85	27.90	28.06
1.30	0.50	2.55	234.63	231.75	1.04	4.36	174.03	173.63	7.26	89.55	89.10	89.11
2.58	3.83	2.54	429.97	429.96	3.96	2.64	274.02	274.60	11.20	124.72	126.39	126.85
5.14	4.85	4.65	104.91	91.54	6.20	6.21	111.51	104.58	12.62	114.25	92.58	92.43
10.26	3.05	3.25	3.15	3.62	4.51	4.89	4.68	5.41	6.86	32.37	11.21	11.43
20.50	0.43	0.60	4.18	4.43	1.14	1.30	7.97	8.42	3.20	5.07	19.24	20.16
36.50	0.88	0.86	1.81	1.92	0.98	1.03	3.94	4.16	3.58	10.12	14.81	15.39
52.50	0.65	0.71	0.20	0.17	0.88	0.97	0.36	0.43	1.82	3.50	5.48	5.83
68.50	0.16	0.22	0.65	0.65	0.28	0.35	1.01	1.00	0.41	1.60	1.25	1.28
84.50	0.07	0.04	0.30	0.31	0.07	0.04	0.55	0.56	0.35	1.50	1.20	1.14
100.50	0.07	0.07	0.02	0.03	0.09	0.09	0.07	0.08	0.21	0.47	0.49	0.47
116.50	0.02	0.03	0.03	0.04	0.04	0.04	0.07	0.06	0.06	0.16	0.11	0.10
132.50	0.00	0.00	0.06	0.07	0.00	0.00	0.07	0.07	0.03	0.15	0.11	0.11
148.50	0.01	0.00	0.06	0.05	0.01	0.01	0.08	0.09	0.02	0.05	0.06	0.07
164.50	0.00	0.00	0.02	0.05	0.00	0.00	0.03	0.05	0.01	0.02	0.02	0.02

Table S6: Coefficient of variance percentage of the optimized leaf-inspired design under fully developed laminar flow for various DNA target concentrations (100, 50, 10, 1 nM) under different flow rates (100, 50, 10  $\mu\text{L}/\text{min}$ ).

Optimized leaf Time (min)	100 $\mu\text{L}/\text{min}$				50 $\mu\text{L}/\text{min}$				10 $\mu\text{L}/\text{min}$			
	100 nM	50 nM	10 nM	1 nM	100 nM	50 nM	10 nM	1 nM	100 nM	50 nM	10 nM	1 nM
0.34	12.62	23.14	69.54	12.75	24.40	23.44	23.29	23.14	70.47	69.97	69.75	69.54
0.66	1.26	5.54	45.86	1.58	5.75	5.48	5.51	5.54	45.85	46.07	45.96	45.86
1.30	0.65	1.74	21.49	161.24	121.82	121.83	5.17	1.74	58.98	59.15	59.39	21.49
2.58	4.25	3.94	13.96	320.01	183.11	182.86	3.12	3.94	84.34	83.98	82.58	13.96
5.14	6.09	6.25	17.62	87.81	92.65	95.44	6.22	6.25	65.39	64.98	63.64	17.62
10.26	4.05	4.96	12.80	4.80	6.01	5.11	5.33	4.96	19.63	19.17	17.59	12.80
20.50	0.79	1.74	5.49	6.82	12.34	11.72	1.83	1.74	19.83	18.94	16.05	5.49
36.50	0.98	0.90	4.77	3.22	6.70	6.39	0.93	0.90	16.60	15.96	13.95	4.77
52.50	0.80	0.86	3.06	0.32	1.28	1.16	0.95	0.86	7.48	7.06	5.79	3.06
68.50	0.23	0.33	0.97	0.78	1.02	1.04	0.40	0.33	2.04	1.87	1.43	0.97
84.50	0.06	0.06	0.39	0.43	0.69	0.69	0.07	0.06	0.84	0.90	1.07	0.39
100.50	0.08	0.09	0.32	0.09	0.12	0.12	0.08	0.09	0.38	0.43	0.52	0.32
116.50	0.03	0.04	0.12	0.08	0.12	0.11	0.04	0.04	0.14	0.14	0.15	0.12
132.50	0.00	0.01	0.03	0.08	0.08	0.07	0.01	0.01	0.13	0.12	0.11	0.03
148.50	0.01	0.01	0.03	0.08	0.09	0.09	0.01	0.01	0.09	0.08	0.06	0.03
164.50	0.00	0.00	0.01	0.04	0.05	0.04	0.01	0.00	0.06	0.04	0.02	0.01

Table S7: Coefficient of variance percentage of the original spine-inspired and optimized leaf-inspired design under fully developed laminar flow for high and low probe densities for a target of 100 nM under flow rate of 100  $\mu\text{L}/\text{min}$ .

Time (min)	Original Spine		Optimized leaf	
	Low: $4.55 \times 10^{11}$ molecules/cm <sup>2</sup>	High: $4.55 \times 10^{13}$ molecules/cm <sup>2</sup>	Low: $4.55 \times 10^{11}$ molecules/cm <sup>2</sup>	High: $4.55 \times 10^{13}$ molecules/cm <sup>2</sup>
0.34	7.91	0.13	0.17	0.18
0.66	0.73	0.02	0.05	0.07
1.30	0.42	0.11	0.05	0.06
2.58	3.71	0.81	0.72	0.80
5.14	4.74	1.96	2.07	2.17
10.26	2.98	2.18	2.43	2.58
20.50	0.42	0.52	0.71	0.85
36.50	0.85	1.11	1.06	1.16
52.50	0.63	0.91	0.85	1.06
68.50	0.15	0.29	0.24	0.38
84.50	0.07	0.05	0.07	0.04
100.50	0.07	0.10	0.08	0.11
116.50	0.02	0.05	0.03	0.06
132.50	0.00	0.01	0.00	0.01
148.50	0.01	0.01	0.01	0.01
164.50	0.00	0.01	0.00	0.01

Table S8: Coefficient of variance percentage of the original spine-inspired and optimized leaf-inspired design under fully developed laminar flow in complex media (plasma, whole blood, and saliva) for a target of 100 nM under flow rate of 100  $\mu\text{L}/\text{min}$ .

Time (min)	Original Spine			Optimized leaf		
	Plasma	Blood	Saliva	Plasma	Blood	Saliva
0.34	10.90	14.48	15.88	22.35	32.68	36.32
0.66	0.58	2.16	2.96	10.61	21.79	25.45
1.30	0.91	1.66	2.03	7.41	17.21	20.40
2.58	4.64	5.29	5.58	10.13	17.56	19.94
5.14	5.84	6.69	7.00	10.80	17.16	19.44
10.26	3.68	4.38	4.65	7.63	13.27	15.49
20.50	0.61	0.93	1.07	3.01	7.41	9.32
36.50	1.05	1.16	1.20	0.93	2.14	3.34
52.50	0.87	1.13	1.23	1.97	2.08	1.98
68.50	0.27	0.46	0.54	1.69	3.00	3.20
84.50	0.06	0.04	0.05	0.79	2.49	3.03
100.50	0.10	0.15	0.16	0.15	1.26	1.86
116.50	0.05	0.09	0.11	0.37	0.46	0.73
132.50	0.00	0.02	0.03	0.33	0.71	0.71
148.50	0.01	0.01	0.01	0.16	0.72	0.85
164.50	0.01	0.01	0.02	0.04	0.48	0.69

## Supplementary figures

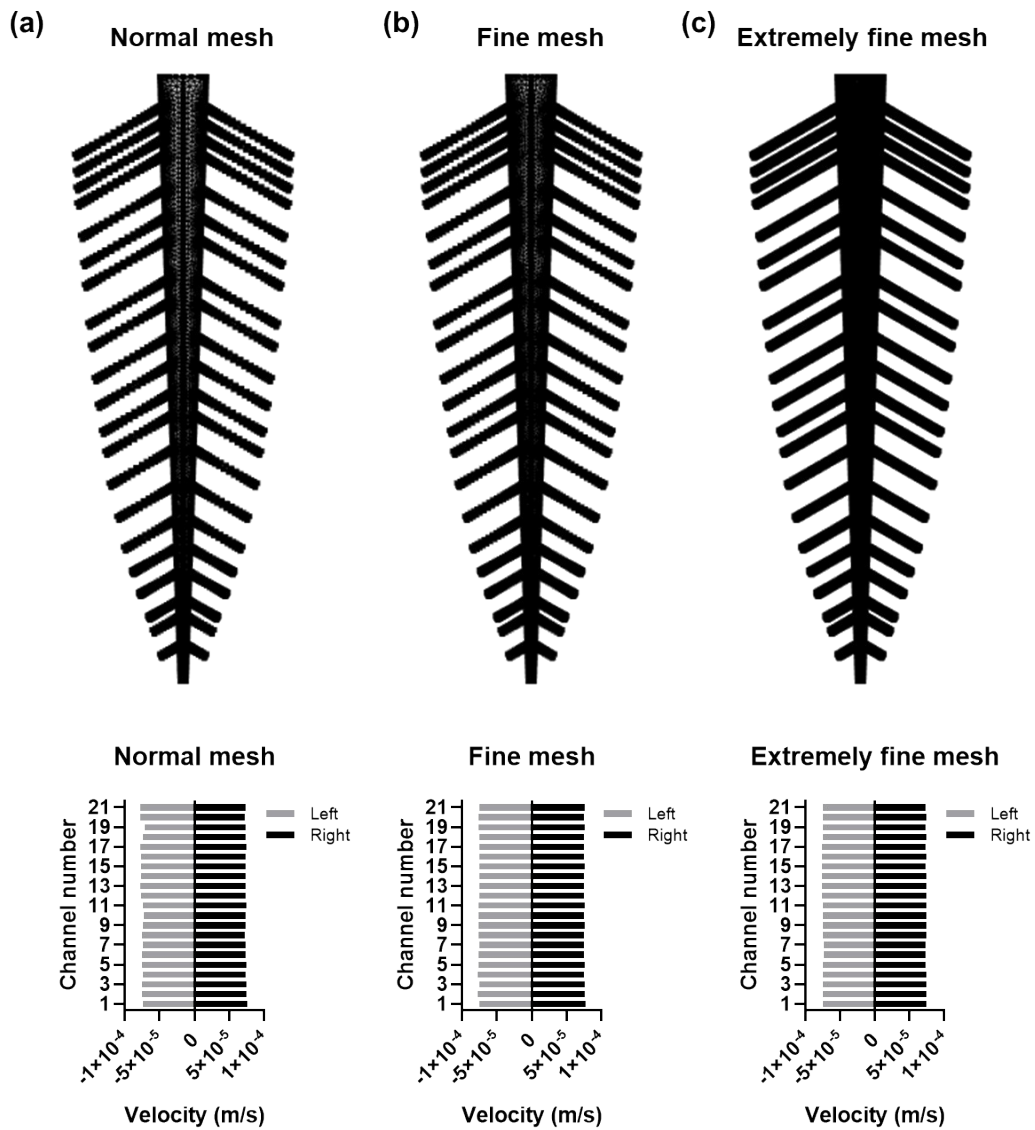


Fig. S1: Meshing analysis of the optimized leaf-inspired design across 42 sub-channel reaction sites. (a) Normal mesh velocity vector measurement (coefficient of variance, 2.4 %). (b) Fine mesh velocity vector measurement (coefficient of variance, 0.86%). (c) Extremely fine mesh velocity vector measurement (coefficient of variance, 0.86 %). Inlet flow rate is set at 100  $\mu$ L/min.

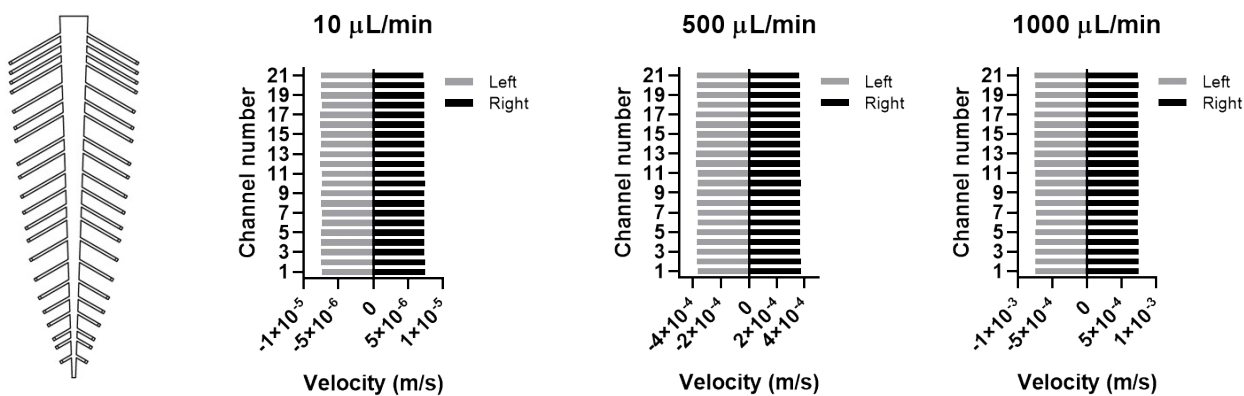


Fig. S2: Meshing analysis of the optimized leaf-inspired design across 42 sub-channel reaction sites. Fine mesh velocity vector measurement (coefficient of variance, 0.86 %) under various inlet flow rates (10 – 1000  $\mu\text{L}/\text{min}$ ).

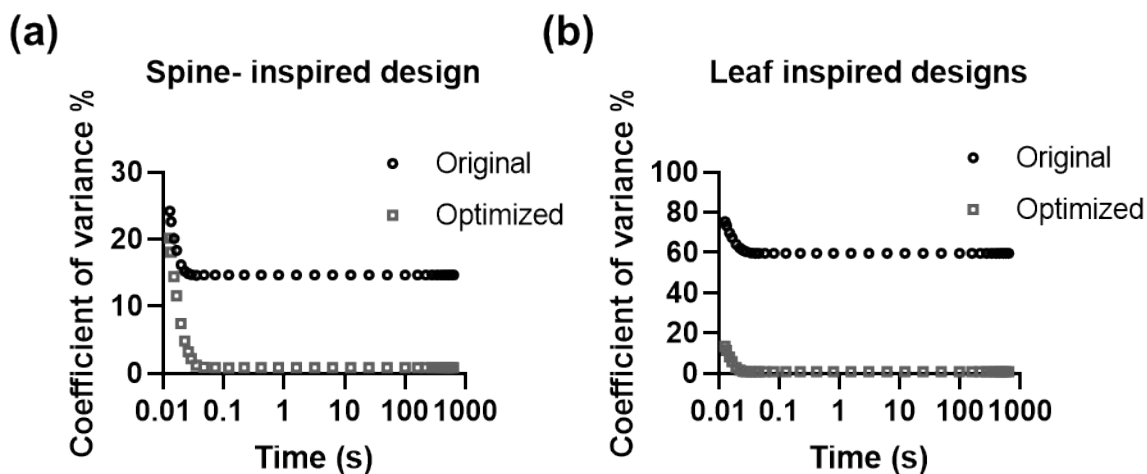


Fig. S3: Coefficient of variance analysis of the velocity vector at the reaction sites of (a) Spine-inspired and (b) Leaf-inspired designs. Simulations are run using fully developed laminar flow under a flow rate of 100  $\mu\text{L}/\text{min}$ .

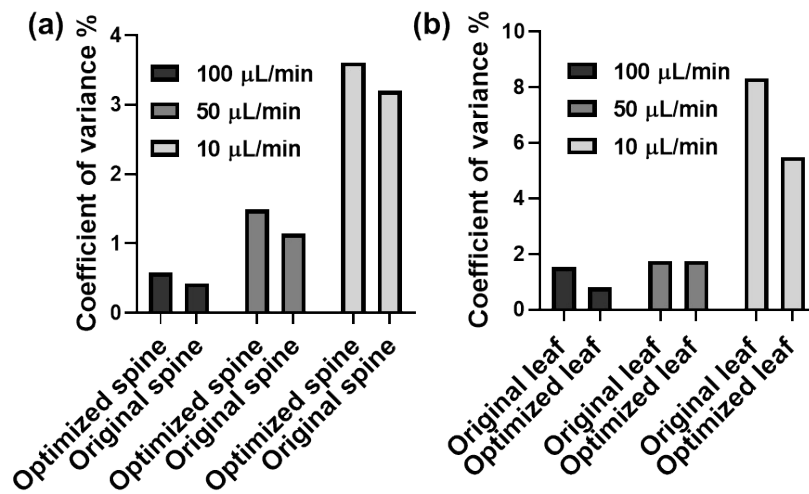


Fig. S4: Coefficient of variance analysis of the bio-inspired designs. (a) Spine-inspired coefficient of variance percentage of the flowing DNA target and capture at the 38 reaction sites. (b) Leaf-inspired coefficient of variance percentage of the flowing DNA target and capture at the 42 reaction sites. Simulations are run using fully developed laminar flow for a DNA target concentration of 100 nM under different flow rates (10, 50, 100  $\mu\text{L}/\text{min}$ ) at 20 minutes.

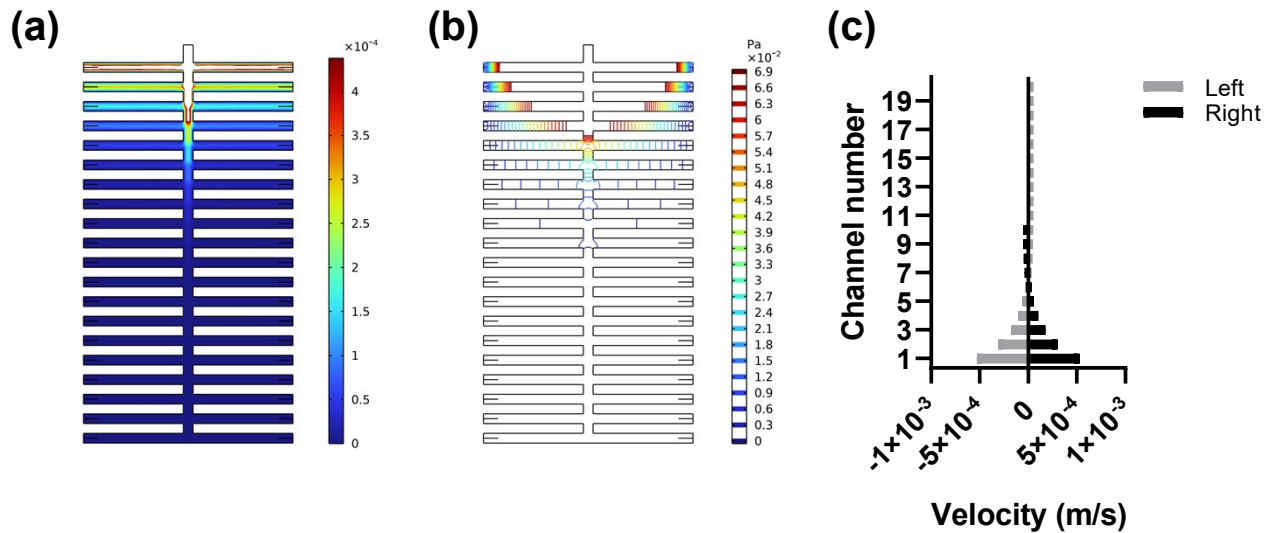


Fig. S5: Analysis of the simple branched design. (a) Velocity profile, (b) Pressure profile, (c) Velocity vector in all 40 sub-channels. Simulations are run using fully developed laminar flow at 100  $\mu\text{L}/\text{min}$ .

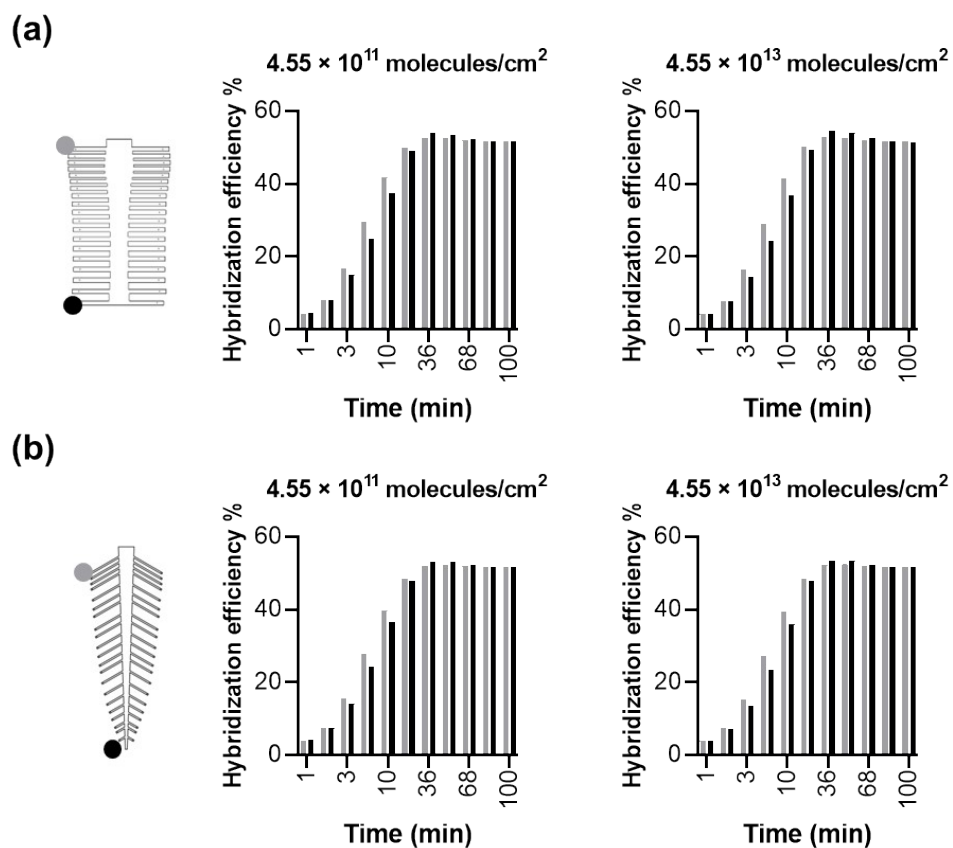


Fig. S6: Effect of probe density on DNA-DNA hybridization of the bio-inspired designs. (a) Hybridization efficiency of the original spine design for the first (gray) and last (black) reaction site. (b) Hybridization efficiency of the optimized leaf designs for the first (gray) and last (black) reaction site. Simulations were set for a target concentration of 100 nM at a flow rate of 100  $\mu$ L/min.

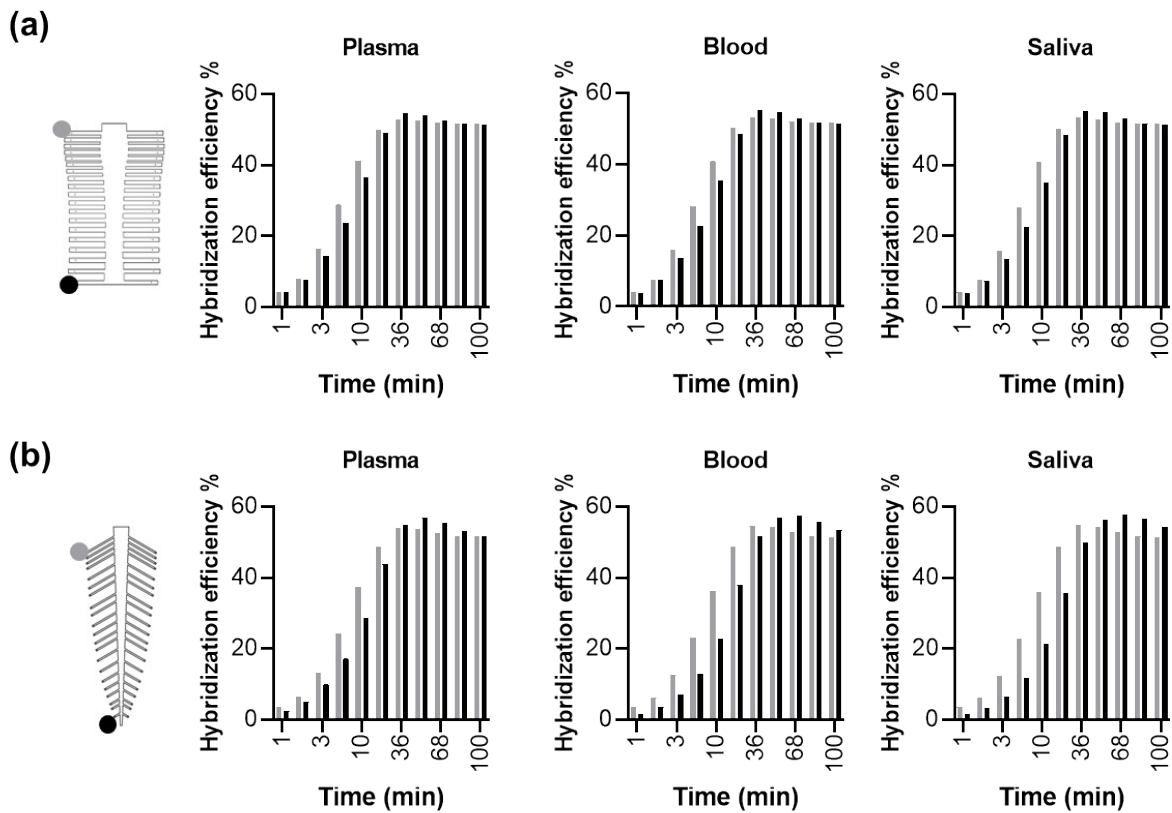


Fig. S7: Effect of complex media (plasma, whole blood, saliva) on DNA-DNA hybridization of the bio-inspired designs. (a) Hybridization efficiency of the original spine design for the first (gray) and last (black) reaction site. (b) Hybridization efficiency of the optimized leaf design for the first (gray) and last (black) reaction site. Simulations were set for a target concentration of 100 nM at a flow rate of 100  $\mu\text{L}/\text{min}$ .

## References

1. COMSOL Multiphysics® v. 6.2. COMSOL AB, Stockholm, Sweden.
2. I. Avramov, *Journal of Non-Crystalline Solids*, 2009, **355**, 745-747.
3. T. Cholko and C.-E. A. Chang, *The Journal of Physical Chemistry B*, 2021, **125**, 1746-1754.
4. J. Chou, L. E. Li, E. Kulla, N. Christodoulides, P. N. Floriano and J. T. McDevitt, *Lab on a Chip*, 2012, **12**, 5249.
5. A. Laribi, S. Allegra, M. Souiri, R. Mzoughi, A. Othmane and F. Girardot, *Talanta*, 2020, **215**, 120904.
6. E. Osman, S. Sakib, R. Maclachlan, S. Saxena, A. A. Akhlaghi, B. R. Adhikari, Z. Zhang, Y. Li and L. Soleymani, *ACS Sensors*, 2024, **9**, 4599-4607.
7. P. Nithiarasu, *Chapter*, 2022, **2**, 20-21.
8. A. A. Mishra, U. Almhöjd, H. Çevik-Aras, A. Fisic, R. Olofsson, A. Almståhl and R. Kádár, *Physics of Fluids*, 2025, **37**.
9. E. Kubala, P. Strzelecka, M. Grzegocka, D. Lietz-Kijak, H. Gronwald, P. Skomro and E. Kijak, *BioMed Research International*, 2018, **2018**, 1-13.